Biochimica et Biophysica Acta, 1064 (1991) 297–307

ADONIS 000527369100200Y

BBAMEM 75233

Palmitate binding to and efflux kinetics from human erythrocyte ghost

Inge N. Bojesen and Eigil Bojesen

Department of Biochemistry B, University of Copenhagen-Panum Institute, Copenhagen (Denmark)

(Received 8 November 1990)

Key words: Palmitic acid transport; Erythrocyte ghost; Efflux kinetics

At 0°C, pH 7.3, palmitate (PA) binds to human erythrocyte ghosts suspended in 0.2% bovine serum albumin (BSA) solution with molar ratios of PA to BSA, ν, between 0.2 and 1.3. The binding depends on the water phase PA concentration, measured in equilibrium experiments, using BSA-filled ghosts as semipermeable bags. The saturable binding has a capacity of 19.4 ± 7.5 nmol g^{-1} packed ghosts ($7.2 \cdot 10^9$ cells) and $K_d = 13.5 \pm 5$ nM. PA exchange efflux kinetics to 0.2% BSA is recorded from ghosts without and with 0.2% BSA with a resolution time of about 1 s. Data are analyzed in terms of compartmental models. Using BSA-free ghosts the kinetics is essentially monoexponential. The rate constant is 0.0287 ± 0.0022 s^{-1}. Using ghosts with BSA, the kinetics is biexponential with widely different rate constants. Extrapolated zero-time values reflect, according to additional investigations, 'instantaneous' release of PA from the outer surface of the ghosts. Analyses of the biexponential curve up to about 55% tracer efflux assign unequivocally values to three model parameters. (1) k_1, the dissociation rate constant of the PA-BSA complex is $(1.47 \pm 0.03) \cdot 10^{-3}$ s^{-1} and $(2.56 \pm 0.08) \cdot 10^{-3}$ s^{-1} and $(4.08 \pm 0.13) \cdot 10^{-3}$ s^{-1} at $\nu = 0.2$, 0.6 and 1.4, respectively. (2) k_3^e, the overall rate constant of PA transport from the inside of the ghost membrane to the medium is 0.0269 ± 0.0020 s^{-1} independent of ν. (3) Q_{kin}, the ratio of PA on the inside of the membrane to PA on BSA within the ghosts is ν dependent and smaller than a corresponding ratio Q_{eq} measured in equilibrium by a value corresponding to PA on the outer surface. This fraction is released with a rate constant, k_5, which is of the order of 1 s^{-1}. The data suggest a maximum PA transport capacity, $J_{\max}$, of 2 pmol min^{-1} cm^{-2}, 0°C, pH 7.3.

Introduction

Our interest in the transport of long-chain fatty acids across cell membranes comes from investigations of the control of prostaglanding production in the renal inner medulla [1]. A complete account of the subject is impossible, because we do not know whether membrane transfer participates in the control of the intracellular level of the prostaglandin precursor, arachidonic acid. From the prostaglandin research we have also hints of the permeation mechanism of long-chain fatty acids. Rabbit erythrocytes are completely impermeable to prostaglandins E_1 and $F_{2\alpha}$, which are only slightly more hydrophilic than unsaturated long chain fatty acids [2]. This speaks against a trivial water-lipid bilayer partition as the basis mechanism for the extremely fast uptake in many cells of long-chain fatty acids. Recent works on the uptake of fatty acid in adipocytes [3,4], cardiomyocytes [5,6] and hepatocytes [7] corroborate this point of view by indicating a carrier-mediated membrane transfer.

We have turned our attention to the human erythrocyte ghosts in order to obtain information on some basic features of the long-chain fatty acid permeation through cell membranes. The fatty acids are not metabolized by erythrocytes except in acylation cycles. Thus it is not very likely that the cells are well equipped with any specific transfer mechanism. The permeation may therefore be slow. On the other hand, the anion transporter is an important fraction of the ghost proteins and a specific inhibitor of anion transport has been reported to inhibit the fatty acid uptake in adipocytes [3]. Fatty acid transport through the ghost membrane is readily investigated because ghosts can be filled with an albumin solution and a reliable technique is available to record rapid efflux kinetics. In addition, the protein-filled ghosts may be an ideal tool to measure

Correspondence: I.N. Bojesen, Department of Biochemistry B, University of Copenhagen - Panum Institute, 3, Blegdamsvej, DK-2200 Copenhagen N, Denmark.

equilibrium constants of fatty acid-protein bindings since the large number of small semipermeable bags ascertain fast equilibrium with external buffers.

A preliminary report on our studies has been published [8] and a related work with oleic acid has appeared [9]. This will be discussed later.

We show that the ghost membrane binds palmitate almost as well as albumin and that the binder participates in the transfer of palmitate across the membrane. In equilibrium, the major fraction of bound palmitate is on the inside of the membrane and thus there is also asymmetry with regard to rate constants of the unidirectional fluxes. The rate constant of transfer from the inside to the medium is the same whether the ghost contain albumin or not and the flux is the product of a v-independent rate constant and a v-dependent occupancy of the 'binder' at the inside of the membrane.

Materials

[(9.10)-^{3}H]Palmitic acid (specific activity 54 Ci/mmol) was obtained from Amersham Int. plc, Amersham, U.K. Unlabelled palmitic acid was obtained from Sigma. Tracer palmitic acid was purified every half a year by chromatography on a silicic column using 2% ethyl acetate in benzene as eluant. Within this period no impurities could be detected.

Bovine serum albumin (BSA) (Behring Institute, Germany) was defatted according to the method of Chen [10]. ^{125}I-labelled albumin was prepared by the radioiodination method using Iodogen as described by Markwell and Fox [11]. Purification of obtained ^{125}I-BSA was carried out by gel-filtration chromatography on a small Sephadex G-25 column (9.1 ml, 5 cm). 95% was trichloroacetic acid precipitable (specific activity 0.135 μCi/μg). Defatted BSA was added to a working solution of ^{125}I-BSA in 165 mM KCl to a specific activity 4.4 nCi/mg.

Methods

The model accounting for tracer palmitate efflux from albumin-free ghost in non-isotopic equilibrium with the medium, containing 0.2% BSA

In exchange flux the net flux of tracer between two subsequent compartments of palmitate is the product of the unidirectional flux of palmitate and the difference in specific activities. Therefore the system kinetics is described by the following first-order linear differential equations, expressed in first-order rate constants k_3 and k_5 (see Fig. 1A for notations)

$$-db/dt = k_3 B(b/B - e/E) \quad (1)$$

$$dy/dt = k_5 E(e/E - y/Y) \quad (2)$$

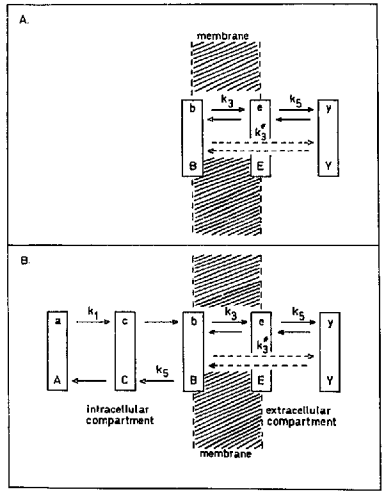

Fig. 1. The models, used to account for the efflux of [^{3}H]palmitate from ghosts in non-isotopic equilibrium with the medium. (Panel A) Ghost without serum albumin. (Panel B) Ghost with serum albumin. Arrows indicate unidirectional palmitate fluxes. k_1, k_3, and k_5 are first-order rate constants of fluxes between adjacent compartments and k_3^* is the rate constant of the unidirectional flux from the membrane inner surface to the medium through the palmitate pool at the membrane outer surface. *a* and *A*: The amount of [^{3}H]palmitate and palmitate bound to intracellular albumin. *c* and *C*: The amount of [^{3}H]palmitate and palmitate in the intracellular water-phase. *b* and *B*: The amount of [^{3}H]palmitate and palmitate bound to the inner surface of the ghost membrane (the transport pool). *e* and *E*: The amount of [^{3}H]palmitate and palmitate bound to the outer surface of ghost membrane. *y* and *Y*: The amount of [^{3}H]palmitate and palmitate in the extracellular medium.

The system is conservative, i.e., the total amount of tracer T, is the sum of the three variables y, b and e.

$$T = y + b + e \quad (3)$$

The volume of the medium is 300–400-fold greater than the ghost volume, therefore (Fig. 1A)

$$Y > (B + E) \cdot 10^2$$

Since B and E are of the same order of magnitude, we have

$$B/Y \ll 1 \text{ and } E/Y \ll 1$$

By rearrangement of Eqn. 2 we get

$$e = (1/k_5)\,\mathrm{d}y/\mathrm{d}t + (E/Y)\,y \tag{2.1}$$

From Eqn. 3 and $E/Y \ll 1$, it follows that

$$b = T - y - (1/k_5)\,\mathrm{d}y/\mathrm{d}t \tag{3.1}$$

and by differentiation

$$-\mathrm{d}b/\mathrm{d}t = \mathrm{d}y/\mathrm{d}t + (1/k_5)\,\mathrm{d}^2y/\mathrm{d}t^2 \tag{3.2}$$

By substituting Eqns. 2.1, 3.1 and 3.2 into Eqn. 1 and using $B/Y \ll 1$ we get

$$\mathrm{d}^2y/\mathrm{d}t^2 + (k_5 + k_3(1 + B/E))\,\mathrm{d}y/\mathrm{d}t + k_5k_3y = Tk_5k_3$$

with the solution

$$(1 - y/y_\infty) = -C1\cdot e^{-\alpha t} - C2\cdot e^{-\beta t} \tag{4}$$

where in isotopic equilibrium ($t = \infty$) $T = y_\infty$ and $Y \gg (B + E)$. The constants C1, C2, α and β are related to the theoretical constants k_3, k_5 and B/E by:

$$C1 + C2 = -1 \tag{4.1}$$

$$\alpha + \beta = k_5 + k_3(1 + B/E) \tag{4.2}$$

$$\alpha\cdot\beta = k_5\cdot k_3 \tag{4.3}$$

and

$$(B/E + 1) = -k_5/(\alpha C1 + \beta C2) \tag{4.4}$$

The latter equation is obtained as follows: Using the differentiated Eqn. 4 we can write

$$\mathrm{d}(y/y_\infty)/\mathrm{d}t \to -(\alpha C1 + \beta C2) \text{ for } t \to 0$$

where $y_\infty = (b_0 + e_0)$ at time zero. Therefore

$$\mathrm{d}y/\mathrm{d}t \to -(\alpha C1 + \beta C2)(b_0 + e_0) \text{ for } t \to 0$$

Furthermore

$$\mathrm{d}y/\mathrm{d}t \to k_5\cdot e_0 \text{ for } t \to 0$$

according to Eqn. 2. Since $e_0/E = b_0/B$, we get Eqn. 4.4.

Simplification of the model according to observations obtained in the present study (Fig. 4A)

The theoretical biexponential time course of $(1 - y/y_\infty)$

$$[-\ln(1 - y/y_\infty) = \alpha t - \ln(-C1) + \beta t - \ln(-C2)]$$

is not observed within our time of resolution, 1 s. The tracer efflux follows a monoexponential time course. Therefore α must be much greater than β and $\mathrm{d}^2y/\mathrm{d}t^2 = 0$, which means after 1 s, $\mathrm{d}y/\mathrm{d}t = -\mathrm{d}b/\mathrm{d}t$ and that $e \ll b$ according to Eqns. 3.2 and 3. Subtraction of Eqn. 3.1 from Eqn. 3 gives

$$e = (1/k_5)\,\mathrm{d}y/\mathrm{d}t = (1/k_5)(-\mathrm{d}b/\mathrm{d}t)$$

Substitution of this equation in Eqn. 1 yields

$$-\mathrm{d}b/\mathrm{d}t = [k_5k_3/(k_5 + k_3(B/E))]b = k_3^*\cdot b$$

which defines a new rate constant k_3^* for the overall transfer of tracer from B to Y through the E compartment, after 1 s. With $\alpha \approx k_5 + k_3(1 + B/E)$, β is expressed as $\beta \approx k_5k_3/(k_5 + k_3(1 + B/E))$ according to Eqns. 4.2 and 4.3 and the constant k_3^* is almost identical with β when $k_5 \gg k_3$ and $B/E > 1$. Two important modifications are applicable on the monoexponential tracer efflux after 1 s:

(1) $e \ll b$

(2) $\mathrm{d}y/\mathrm{d}t = -\mathrm{d}b/\mathrm{d}t = k_3^*\cdot b$

The model accounting for tracer palmitate efflux from ghosts containing buffer with 0.2% BSA in non-isotopic equilibrium with a medium containing 0.2% BSA (Fig. 1B)

Some features of the model, accounting for the tracer efflux from ghosts without BSA is directly applicable here since the two systems differ only with regard to the intracellular compartments. Thus we can use, within our time of resolution, 1 s, the modifications (1) $e \ll b$ and (2) $\mathrm{d}y/\mathrm{d}t = k_3^*\cdot b$.

By analogy with the system above, the kinetic equations to describe the intracellular compartments are expressed in first-order rate constants k_1, k_5 and k_3^*:

$$-\mathrm{d}a/\mathrm{d}t = k_1A(a/A - c/C) \tag{5}$$

$$-\mathrm{d}b/\mathrm{d}t = k_3^*b - k_5B(c/C - b/B) \tag{6}$$

By eliminating c/C from Eqns. 5 and 6 we obtain

$$(c/C) = (1/(k_1A))\,\mathrm{d}a/\mathrm{d}t + a/A$$

$$= (1/(k_5B))(k_3^*b + \mathrm{d}b/\mathrm{d}t) + b/B \tag{7}$$

The conservation of the total amount of tracer, T, means that

$$T = y + a + b + c + e$$

Now $c/C \leq a/A$ and $C < 10^{-3}A$ and therefore $c \lll a$ thus

$$T = y + a + b + e$$

The initial tracer of the E compartment, e_0, is transferred to the Y compartment within our resolution time. Therefore, after 1 s efflux

$$T = y + a + b$$

This enables us to express the variables of Eqn. 7 in terms of y by using

$$b = (1/k_3^*)\,\mathrm{d}y/\mathrm{d}t$$

$$\mathrm{d}b/\mathrm{d}t = (1/k_3^*)\,\mathrm{d}^2y/\mathrm{d}t^2$$

$$a = T - y - (1/k_3^*)\,\mathrm{d}y/\mathrm{d}t$$

$$\mathrm{d}a/\mathrm{d}t = -\mathrm{d}y/\mathrm{d}t - (1/k_3^*)\,\mathrm{d}^2y/\mathrm{d}t^2$$

With $Q = B/A$ then Eqn. 7 becomes

$$\mathrm{d}^2y/\mathrm{d}t^2 + \frac{k_3^* + k_5(1+Q) + k_3^* k_5 Q/k_1}{1 + Q\cdot k_5/k_1}\,\mathrm{d}y/\mathrm{d}t + \frac{k_3^* k_5 Q}{1 + Q\cdot k_5/k_1}\,y$$

$$= \frac{k_3^* k_5 Q T}{1 + Q\cdot k_5/k_1}$$

since k_5 is of the order of 1 s^{-1} (see results) and k_1 is at least 300-fold smaller [12], we can neglect 1 compared with Qk_5/k_1, when Q is in the range of 0.1 to 0.5. Therefore the second order differential equation is reduced to

$$\mathrm{d}^2y/\mathrm{d}y^2 + \mathrm{d}y/\mathrm{d}t(k_3^* + k_1(1 + 1/Q)) + yk_1k_3^* = Tk_1k_3^* \qquad (8)$$

with the solution

$$(1 - y/y_\infty) = -C1\,\mathrm{e}^{-\gamma t} - C2\,\mathrm{e}^{-\delta t},\ T = y_\infty \text{ for } t = \infty \qquad (9)$$

where C1 and C2 are integration constants of the homogeneous equation and $-(C1 + C2) + y_0/y_\infty = 1$. With the boundary condition $Q = B/A \to b(t = 0)/a(t = 0)$ for $t \to 0$, the following three equations define the model parameters:

$$k_1 = \gamma\delta/k_3^* \qquad (10)$$

$$k_3^* = \gamma + \delta + \gamma\delta/(\gamma C1 + \delta C2) \qquad (11)$$

$$Q = B/A = \frac{-(\gamma C1 + \delta C2)}{k_3^* + \gamma C1 + \delta C2} \qquad (12)$$

Eqn. 12 is obtained by analogy with obtaining Eqn. 4.4. To distinguish B/A from a related ratio measured in equilibrium experiments, $Q_{eq} = (B + E)/A$, we use the notation $Q_{kin} = B/A$. Thus in theory $Q_{eq} = Q_{kin}(1 + E/B)$.

Data analyses and statistics

The time series of efflux aliquot counting rates are collected directly as data files, using a Hewlett Packard 85B microcomputer. The data of experiments with albumin-filled ghosts are analyzed with this machine according to Eqn. 9, using the 'exponential stripping' method [13]. The experimental uncertainties of computed parameters of single experiments are computed according to the previously described principle [14] involving independent contributions to the error and numerical differentiation. The presented mean values of parameters are calculated from single experimental values for which the uncertainties are at the same level.

For the Gauss-Newton least-squares curve fitting [15] is used an Olivetti M-28 computer.

Student's t-test for unpaired values is used to estimate the significance of differences of two means.

Preparation of resealed ghosts

The technique for preparing a uniform population of resealed 'pink' ghosts was based on the directions given by Schwoch and Passow [16] carried out as described by Funder and Wieth [17]. Heparinized human blood from six donors form the basis of the experiments. The erythrocytes were washed with KCl solution (165 mM) and cooled to 0 °C, 1 volume suspension (haematocrit 40%) was added to 10 volumes haemolysing solution: 3.8 mM acetic acid, 4 mM $MgSO_4$, 0.5 mM EGTA: EDTA 1 : 1, 0 °C and pH 3.4–3.6. The pH hereby increases to 6.0. 5 min later 1 volume 2 M KCl containing 25 mM Trizma base (Sigma) was added, changing the pH to 7.3. After further 10 min at 0 °C the lysate was transferred to 38 °C for 45 min and the ghosts reseal. The resealed ghosts were isolated by centrifugation 20 000 × g for 5 min at 0 °C in an Ultracentrifuge model L5-65 (Beckman) Rotor TY 65 and washed in 165 mM KCl, 2 mM phosphate buffer (pH = 7.3, 0 °C) containing 0.02 mM EGTA : EDTA 1 : 1.

The preparation of resealed ghost with intracellular BSA was in all cases carried out by adding 0.2% BSA to the haemolysing solution. Addition of ^{125}I-BSA to the lysate was found to have reached 93.8 ± 1.7% ($n = 9$) equilibration with the intracellular phase of resealed ghosts. The haemolysing solution containing 0.2% BSA has a pH of 4.3 and pH was increased to 6.0–6.2 with the erythrocyte suspension.

For storage, the ghosts were resuspended in the washing buffer containing 0.2% BSA to a cytocrit of 0.36. Such ghosts are well suited for experiments at least two days when kept at 0 °C.

Haemoglobin in ghosts was analyzed according to Van Kampen and Zijlstra [18]. 3.4% of the initial haemoglobin remains in the ghosts. Counting of cells for experiments was carried out in 165 mM KCl solution containing 0.2% BSA on a Coulter Multisizer with a sampling stand with 70 μm orifice. Mean ghost area was 144 μm^2/cell calculated by the Multisizer on basis of mean volume of cells.

Preparation of charge buffers and labelling of resealed ghosts

Media for labelling of ghosts, charge buffers, were prepared as described by Bojesen [19]. Labelled and unlabelled palmitate was deposited on small glass spheres and adsorbed to defatted albumin by gentle shaking 15 min at 37°C. Such media with pH 7.3 contain 165 mM KCl, 2 mM phosphate, 0.2% BSA and 0.6–1 μCi/ml of palmitate. Ghosts were gently packed 5 min by centrifugation at 22200 rpm (36500 × g) at 0°C in a Cryofuge 6-4 (Heraeus Christ).

Equilibration of fatty acid between charge buffer and packed ghosts (1.5 : 1, v/v) was completed by incubation 50 min at 0°C. The labelled ghosts were separated from the charge buffer by centrifugation in a Cryofuge 6-4 (Heraeus Christ) 5 min, 0°C at 22200 rpm (36500 × g) and washed four times with 5 ml 165 mM KCl, 2 mM phosphate buffer at 0°C.

Uptake of palmitate by ghosts

The extracellular volume trapped by the packed cells was 20% ± 2% as evaluated by the ^{125}I-BSA space [20]. 750 μl charge buffer was added 500 mg (μl) packed BSA-free ghosts and the uptake (M) of palmitate by the ghosts is calculated from the counting rate/μl of the charge buffer before (R_1) and after (R_2) equilibration with the ghosts and the specific activity (S, counting rate/nmol) of palmitate as

$$M = (R_1 \cdot 750 - R_2(750 + 0.2 \cdot 500))/(0.8 \cdot 500 \cdot S) \; (nmol/mg)$$

The final ν of the charge buffer is $R_2(750 + 0.2 \cdot 500)/(S \cdot P)$ where P is the amount of albumin of the charge buffer.

Water phase palmitate concentrations F in equilibrium with albumin bound palmitate

BSA-filled ghosts were labelled to various ν values with charge buffer (1 : 1.5, v/v). After removal of charge buffer, the ghosts were washed 4–5-times with ten volumes 165 mM KCl, 2 mM phosphate buffer (pH 7.3) containing 0.02 mM EGTA : EDTA 1 : 1 at 0°C and 400 μl cell free supernatant was taken for counting after centrifugation. This procedure removes virtually no palmitate from the ghosts in agreement with the low equilibrium constant of BSA binding, about 10^{-8} M. F was calculated from counting rate of the supernatant and the specific activity of palmitate. The corresponding intracellular ν was calculated as above, with correction for M or directly from R_2 as $\nu = (R_2 \cdot 1000/S)/29.85$ where 29.85 nmol/ml is the concentration of 0.2% BSA.

Efflux experiments

Washed labelled ghosts packed by centrifugation at 0°C for 15 min at 50000 × g in plasic tubes (i.d. 3 mm) were used for efflux experiments. The supernatant was removed by cutting the tube just below the interface. 100–140 μl packed (about $(7.5–10.5) \cdot 10^8$ cells) ghosts were injected into 30–40 ml stirred isotope-free 165 mM KCl, 2 mM phosphate medium, 0°C, (pH 7.3), containing 0.2% BSA with unlabelled palmitate. Serial sampling of cell-free extracellular medium was done with the Millipore-Swinnex filtration technique [21]. 10–15 samples (including an equilibrium sample) were taken at appropriate intervals for determination of the extracellular accumulation of radioactivity as a function of time. The activity of filtrates was measured by counting 400 μl in 3.9 ml OPTI-FLUOR scintillation fluid.

The effect of DIDS (4,4′-diisothiocyano-2,2′-stilbenedisulphonic acid) was studied by treating the ghosts with 50 μM DIDS solution for 45 min at 38°C as described by Funder and Wieth [17]. After centrifugation and removal of the DIDS solution, the ghosts were labelled and the efflux was determined in a DIDS-free as well as in a 80 μM DIDS medium, which is 2.7-times the concentration of BSA (30 μM).

Results

Binding of palmitate to the ghost membrane

In order to express the binding to the membrane as a function of the water phase palmitate concentration

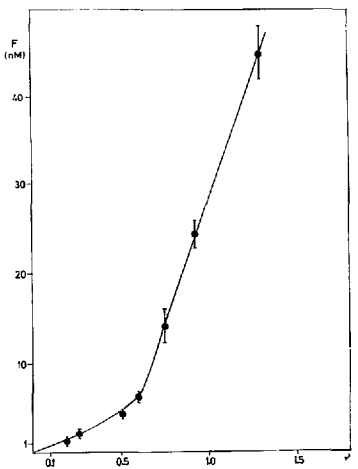

Fig. 2. The relationship between water-phase concentration of palmitate at 0°C (F) and molar ratio of palmitate to albumin (ν) in ghosts for $\nu < 1.3$. Each point is the mean ± S.E. of 6–9 estimates. The curve is drawn by hand.

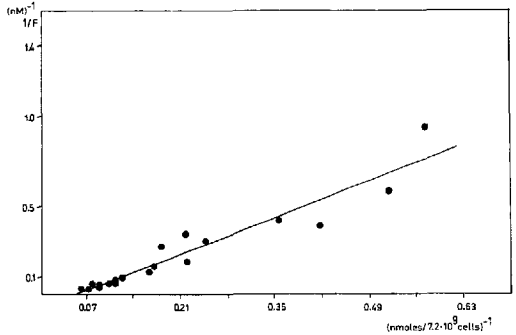

Fig. 3. A plot of $1/F$ versus the reciprocal value of palmitate bound to BSA-free erythrocyte ghosts (nmol/g packed ghosts per $7.2 \cdot 10^9$ cells) at 0°C. Palmitate bound to the ghosts is calculated from the uptake on ghosts added to a 0.2% BSA medium with [^{3}H]palmitate. The water-phase concentrations (F) are obtained from Fig. 2 using the calculated final ν values. The regression line is: $Y = 1.44\ (\pm 0.1)X - 0.074\ (\pm 0.027)$, $r = 0.96$, $t = 13.7$, $n = 19$. Each point represents duplicate determinations.

(F), values of F were measured at different ν values (0.2–1.3) at 0°C (pH 7.3). The results, obtained with BSA-filled ghosts are presented in Fig. 2. The relationship is not analyzed in terms of 'binding sites' but the curve obviously corroborates the presence of multiple fatty acid-binding sited of BSA [22,23].

The palmitate uptake by BSA-free ghosts, equilibrated with charge buffers at various ν values, can now be expressed in terms of F. The experimental procedure and the way of calculation is presented in Methods. If the binding is saturable with only one equilibrium constant, then the plot of $1/F$ versus the reciprocal value of bound palmitate will be linear. The data of Fig. 3 show that the plot is linear and the slope gives the ratio of binding capacity to K_d and the intercept with the ordinate gives $-1/K_d$. In terms of the model (Fig. 1) the binding capacity is the maximum value of $(B+E)$ and amounts to 19.4 ± 7.3 nmol g^{-1} packed ghosts and K_d is 13.5 ± 5 nM according to linear regression. According to a Wilkinson plot [24] the capacity is 21.2 ± 2.1 nmol g^{-1} packed ghosts and $K_d = 16.0 \pm 1.4$ nM.

The uptake data can also be used to calculate an equilibrium ratio $Q_{eq} = (B+E)/A$ (see Fig. 1). The calculation requires knowledge of the dry matter of packed ghosts (about 4%) and the intracellular BSA concentration, estimated to 93.8% of 0.2%. Q_{eq} is then the ratio of tracer bound to the ghosts to tracer bound to 93.8% of 0.2% BSA in a volume of the medium equivalent to 96% of ghost volume.

Efflux kinetics of palmitate from ghosts without and with 0.2% BSA

Ghost without BSA. Two to four effluxes are run with the same ghost preparation and the pooled data from such a series are shown in Fig. 4A. The tracer release is fast and results in a fractional efflux of about 50% after less than 20 s. The fractional efflux fit a monoexponential time course up to 80%. The same has been found in two more series. The theoretical biexponential time course (Eqn. 4) has therefore not been detected. The rate constant (α) of the rapid phase of tracer release is high, since this release is almost completed within 1 s. In contrast, the rate constant (β) of the slow phase of tracer release is much smaller. In three series the β values (S.D.) are: 0.0251 (0.0003), 0.0301 (0.0006) and 0.0310 (0.0003) s^{-1}.

The intercept of the regression line (Fig. 4A) reflects the effect of a rapidly released fraction $E/(E+B)$ from the membrane outer surface. It varies considerably between the three series, the values (S.E.) are 0.068 (0.005), 0.165 (0.006) and 0.093 (0.006).

In terms of Eqn. 4 the intercept values are $-\ln(-C2)$ which is insignificantly different from $(-C1)$ according to Eqn. 4.1 when $-C2 > 0.85$. Combining Eqns. 4.2 and 4.4 and knowing that $\alpha \gg \beta$, we get

$$E/(E+B) = (-C1)(1+(k_3(1+B/E))/k_5) + (-C2)\beta$$

which means that

$$E/(E+B) > (-C1) = -\ln(-C2) = 0.11 \text{ (in average)}$$

TABLE I

Model parameters. Dissociation rate constants (k_1) of palmitate-BSA complexes, overall rate constants (k_3^*) of palmitate transport from inner surface of ghost membrane to the medium and the ratios (Q_{kin}) of palmitate associated with membrane inner surface to palmitate on intracellular BSA

The parameters are determined from efflux experiments data and calculated according to Eqns. 10, 11 and 12 (see text). Experiments are carried out in 165 mM KCl, 2 mM phosphate buffer (pH 7.3 at 0°C). The corresponding 'transformed Q_{eq}' values are calculated from Q_{eq} values determined in equilibrium experiments (see text) and presented for comparison with Q_{kin} values.

I. Exponential stripping curve-fitting is used to obtain the coefficients C1, C2, α and β of Eqn. 2.

	k_1 (10^{-3} s^{-1}) mean (S.E.)	k_3^* (10^{-3} s^{-1}) mean (S.E.)	Q_{kin} mean (S.E.)	'Transformed Q_{eq}'
$\nu = 0.2$ ($n = 9$)	1.47 (0.03)	24.0 (1.8)	0.20 (0.01)	0.20
$\nu = 0.6$ ($n = 9$)	2.56 (0.08) [a]	26.8 (1.9) [c]	0.37 (0.01) [a]	0.32 [a]
$\nu = 1.4$ ($n = 4$)	4.08 (0.13) [b]	30.0 (1.4) [c]	0.63 (0.03) [b]	0.56 [b]

II. Comparison of the results of two methods of curve-fitting in some representative experiments.

	k_1 (10^{-3} s^{-1}) mean (S.E.)	k_3^* (10^{-3} s^{-1}) mean (S.E.)	Q_{kin} mean (S.E.)
A. Exponential stripping method			
$\nu = 0.02$ ($n = 3$)	1.54 (0.16)	24.3 (2.0)	0.19 (0.02)
$\nu = 0.6$ ($n = 3$)	2.48 (0.22)	29.0 (2.0)	0.38 (0.04)
B. Gauss-Newton least-squares method			
$\nu = 0.2$ ($n = 3$)	1.59 (0.32)	20.3 (3.5)	0.21 (0.05)
$\nu = 0.6$ ($n = 3$)	2.58 (0.58)	24.5 (4.4)	0.44 (0.13)

[a] Differs from $\nu = 0.2$ data, $P < 0.001$.
[b] Differs from $\nu = 0.6$ data, $P < 0.001$.
[c] None of the k_3^* values are significantly different ($P > 0.05$).

Without measurements of α a quantitative estimation of $E/(E+B)$ is impossible. However, with a 4% bias of $(1 - y_{15}/y_\infty)$ we have $(-C1)\,e^{-\alpha} = 0.04\,(-C2)\,e^{-\beta}$, and with $(-C1) = 0.11$, $(-C2) = 0.89$ and $\beta = 0.029$ s^{-1} we get a minimum value of α of 1.16 s^{-1}. Using Eqns. 4.2, 4.3 and 4.4 and the definition for k_3^*, we obtain the values 0.8 s^{-1}, 0.038 s^{-1}, 5.3 and 0.030 s^{-1} for k_5, k_3, B/E and k_3^*, respectively. Thus $E/(E+B) = 0.16$ for this minimum value of α. Since to a minimum of α corresponds a maximum of k_3/k_5 and a minimum of B/E these values give the greatest difference between β and k_3^* viz. the model predicts no significant difference between β and k_3^*. Noticeable is the agreement of k_3^* calculated from the experimental data with β obtained directly as the slope of the monoexponential efflux from albumin-free ghosts (Table I). The mean values are not significantly different ($P > 0.5$).

Ghosts with 0.2% BSA. On the basis of the results with albumin-free ghosts, we expect that the efflux kinetics fit the biexponential Eqn. 9 after 1 s^{-1}. As shown by Figs. 4B and 4C this is indeed the case. We have limited our analysis to about 55% fractional efflux to minimize any potential effect of k_1 heterogeneity. The values of the three model parameters k_3^*, k_1 and Q_{kin} obtained by analyses of the exchange efflux data at different ν values are presented in Table I.

The method of 'exponential stripping' has been used in most cases but Table I shows that the results obtained with the Gauss-Newton least-squares method are not different.

The extrapolated zero-time fractional tracer release is in general about 6% but varies between 3% and 10%. According to the model on which the analysis is based, this fraction is the tracer fraction on the outside of the ghost membrane at zero time provided other sources have been excluded. The charge buffer was removed from the extracellular space by washing with buffer and rupture of the ghosts when injected into the medium is not a general phenomenon. When ghosts were loaded with ^{125}I-BSA less than 1%, our detection limit, appeared in the efflux.

It is possible to calculate E/B ratios from Q_{kin} values of Table I since at zero time $e_0/(a_0 + b_0 + e_0) = E/(A + B + E) = y_0/y_\infty = 0.06$ and $Q_{kin} = B/A$.

For ν 0.2 and 0.6 we get E/B 0.38 and 0.23, respectively. For albumin-free ghosts our estimate of E/B is 0.19. Therefore there is no reason to believe that E/B depends on the presence of BSA within the ghosts.

With 6% located at the outside we are able to calculate from Q_{eq} a 'transformed Q_{eq}' value equivalent to a Q_{kin} value. The results are presented in Fig. 5 and values corresponding to $\nu = 0.2$, 0.6 and 1.4 are presented in Table I.

Within the investigated range of ν, the k_3^* values are not statistically different in contrast to variations of Q_{kin} and k_1.

Inhibition studies

Treatment of ghosts with DIDS was without any effect on rates of palmitate efflux from BSA-filled ghosts, whether the medium contained DIDS or not

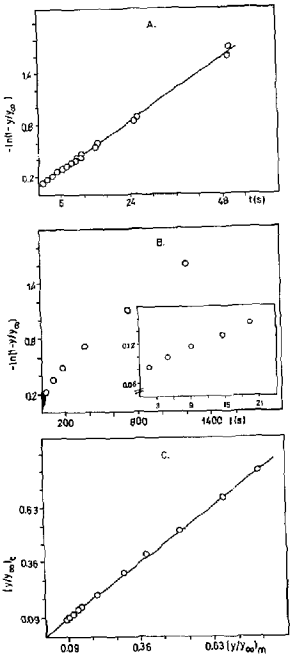

Fig. 4. (A) Exchange efflux kinetics of [^{3}H]palmitate from BSA-free ghosts at 0°C (pH 7.3), ν 0.2 into the extracellular medium. The ghosts were prepared in 165 mM KCl (see Methods) and the medium is 165 mM KCl, 2 mM phosphate buffer containing 0.2% BSA and 0.02 mM EDTA/EGTA (1:1). y is the amount of [^{3}H]palmitate in the medium at the time of sampling and y_∞ is the amount after isotopic equilibrium has been attained. The regression line is $-\ln(1-(y/y_\infty)) = 0.0310\ (\pm 0.0003)t + 0.093\ (\pm 0.006)$, $r = 0.999$, $t = 91$, $n = 22$ (some of the points coincide). (B) Exchange efflux kinetics of [^{3}H]palmitate from ghosts loaded with 0.2% BSA at 0°C (pH 7.3), ν 0.2 into the same medium as described in Fig. 4A. The bar represents five points. y and y_∞ as in Fig. 4A. The inset shows the very early portion of the efflux curve. (C) Test of the analysis using exponential stripping according to Eqn. 9. The data presented in Fig. 4B are used to give the parameters $C1$, $C2$, y_0/y_∞, γ and δ. The figure shows the recalculated $(y/y_\infty)_c$ and measured $(y/y_\infty)_m$ data relationship. The equation of the line is with S.D. values: $(y/y_\infty)_c = 1.001\ (\pm 0.004) \cdot (y/y_\infty)_m + 0.0010\ (\pm 0.0018)$, $r = 0.999$, $t = 224$, $n = 11$.

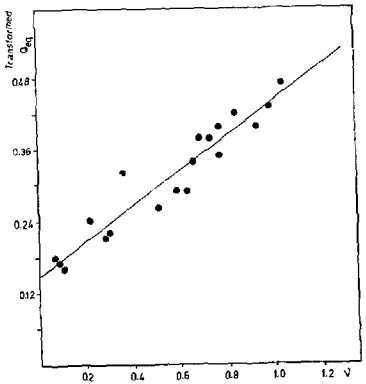

Fig. 5. The ν dependency of the ratio of palmitate bound to the inside of the ghosts to palmitate on intracellular BSA, calculated from equilibrium experiments ("transformed Q_{eq}", see text). The regression line is $y = 0.29\ (\pm 0.022)X + 0.146\ (\pm 0.014)$, $r = 0.96$, $t = 13$, $n = 19$.

(data not shown). The uptake of palmitate after treatment of BSA-filled ghosts 45 min at 38°C with 50 μM DIDS was also unaffected since complete equilibration was achieved at 0°C after 15 min.

Discussion

The transport of the sparsely water soluble long-chain fatty acids through the ghost membrane can only be investigated by means of a device which ascertains well defined water-phase concentrations on both sides of the membrane. Since ghosts are readily supplied with a protein solution when the cells are lyzed, the obvious way of solving the problem is to use an albumin solution of suitable concentration. Preliminary experiments with such a system using 0.2% BSA revealed to our surprise that the exchange efflux kinetics of palmitate after 1 s is clearly biexponential with an initial phase which is too rapid and large to be assigned to dissociation from BSA and/or to the negligeable pool of water phase palmitate. The observation suggested that the rapid phase reflects the efflux of palmitate, bound to the membrane, in agreement with Goodman [25]. A biphasic efflux of oleic acid from ghosts with BSA is published most recently [9] without any attempt to explain the phenomenon although a rapid oleic acid uptake by albumin-free ghosts was observed from a medium with albumin at very low ν.

The palmitate binding depends of course on the water phase concentration at various ν values and the

ν-water phase concentration relationship is in this work determined, for the first time, by using the ghosts as dialysis bags.

The double-reciprocal plot, Fig. 3, strongly suggests that below $\nu = 1.3$ one type of binding sites in the membrane is dominating the uptake. The binding capacity is about 19 nmol per g packed ghosts (about 10^{10} cells). This is similar to the amount of the anion transporter 5–29 nmol per 10^{10} erythrocytes [26] and corresponding to about 150 mol phospholipids per mol palmitate calculated from [27]. Above $\nu = 2$ the uptake is continuously increasing with ν [25] in the same way as described for phospholipid bilayers [28]. Thus the membrane bilayer itself plays probably a small part in the binding when ν is below 2. The preferential binding to the inside of the ghost membrane points in the same direction. The reason for this asymmetry is not known at present.

The membrane binder competes well with BSA as indicated by the 0°C equilibrium constant, $K_d = 13.5$ nM ($K_a = 7.4 \cdot 10^7$ M^{-1}) to compare with K_a $2.9 \cdot 10^7$ M^{-1} for palmitate binding to BSA at 23°C [22] estimated for low ν values and calculated for three binding sites per mol BSA.

Both observations are consistent with the observation of Spector et al. [29] that the erythrocyte membrane contains a relatively small number of sites that bind fatty acids tightly with K_d equal to albumin.

On the other hand there is a large difference between the involved dissociation rate constants. According to our data the dissociation rate constant of the palmitate-membrane binding (k_2) is almost three orders of magnitude greater than the dissociation rate constant of palmitate-albumin binding determined in this study (k_1) and reported values [12,30]. However, the association- and the dissociation rate constants of palmitate–albumin interaction are both exceptionally low and the process of association occurs probably in two steps [12]. The peculiar channel type of the albumin binding sites [31] may account for the very slow on and off type of binding. The two rate constants of the membrane binding may therefore in fact be expected to be much faster.

The model implies that the rate of palmitate dissociation from BSA can be accounted for by a single rate constant. With two or three binding sites per BSA molecule and increasing heterogeneity of the binding with increasing ν [23], we anticipate that a single rate constant describes the process only to a limited extend, even at the investigated low ν values of 0.2 and 0.6.

As shown by the analytical results of Table I, we have chosen a range for which the parameter values are well defined and the same whether they are determined by 'exponential stripping' or by Gauss-Newton least-squares curve-fitting. Furthermore the k_2^* values obtained at 0.2, 0.6 and 1.4 (Table I) are not significantly different from the corresponding β values measured in experiments with BSA-free ghosts and $Q_{\text{lim}} = (B/A)$ is largely in agreement with the equivalent 'transformed Q_{eq}' calculated from Q_{eq} obtained in independent equilibrium experiments (Fig. 5 and Table I).

Table I shows that k_1 increases significantly with ν. Thus we have for the first time demonstrated an effect of ν in the range below 1. The present values are not readily compared with previously published values because different types of albumin, fatty acids, ν values and temperatures have been used. The values reported by Scheider [12] $(2.6–3.7) \cdot 10^{-3}$ s^{-1} obtained for oleate and human serum albumin at 0°C with $\nu = 1$ are comparable to our $k_1 = (2.56 \pm 0.08$ (S.E.)$) \cdot 10^{-3}$ s^{-1} (Table I) at $\nu = 0.6$. Svenson et al. [28] working with

TABLE II

Long chain fatty acid permeation in mammalian cells

Cell type	Temp. (°C)	Fatty acid	Number of cells	V_{max} (nmol min^{-1})	Cell area (μm^2)	V_{max} (pmol min^{-1} cm^{-2})	References
Erythrocyte ghosts	0	16:0 [a]	10^{10}	30 [b]	144	2	this paper
Adipocytes	23	16:0 [a]	$5.5 \cdot 10^4$	2.5	$1.5 \cdot 10^4$ [c]	300	3
	23	18:1 [d]	$5.5 \cdot 10^4$	1.0	$1.5 \cdot 10^4$ [c]	120	3
	37	18:1 [d]	$5.0 \cdot 10^4$	2.5	$1.5 \cdot 10^4$ [c]	330	4
Hepatocytes	37	18:1 [d]	$5.0 \cdot 10^4$	0.2	$1.3 \cdot 10^3$ [e]	300	7
Cardiac myocytes	37	18:1 [d]	$5.0 \cdot 10^4$	0.48–0.59	$1.4 \cdot 10^4$ [f]	68–84	5
	37	18:1 [d]	10^6	1.91	$1.4 \cdot 10^4$ [f]	137	6

[a] Palmitic acid.
[b] The value is the product of the rate constant, k_2^*, and the binding capacity of the membrane (J_{max}).
[c] The adipocytes are assumed to be 70 μm in diameter [37].
[d] Oleic acid.
[e] The hepatocyte is assumed to be 20 μm in diameter [38].
[f] The average dimension of cardiac myocytes is assumed to be 138 $\mu m \cdot 30.5$ μm [39].

human serum albumin and palmitate, $\nu = 0.95$ has obtained a rate constant at 9°C of $10 \cdot 10^{-3}$ s^{-1} to compare with $(10.2 \pm 1.4$ (S.E.)$) \cdot 10^{-3}$ s^{-1} ($n = 7$) obtained with the present technique at 10°C [8]. Extrapolation of their data to 0°C gives $3.98 \cdot 10^{-3}$ s^{-1} which is quite similar to the value obtained in the present study at 0°C.

In the low range of ν our results suggest that the unidirectional flux of palmitate is the product of a ν independent rate constant and the occupancy of the membrane binder. Extrapolation to saturation of the binder gives a calculated maximum flux (J_{max}) of about 2 pmol min^{-1} cm^{-2}, using mean area 144 μm^2/ghost (see Methods). This J_{max} is about 250-fold smaller than for glucose [32]. To get an idea of whether it is large or small for long-chain fatty acids we have compared it with the fatty acid membrane transport into cells which metabolize the fatty acids vigorously (Table II). Although the location of the cell-bound fatty acid has not been identified in any of the uptake studies it is probably membrane translocated acid bound to intracellular adsorbents, since we have experienced that release from membrane binding is very rapid.

For palmitate the about 150-fold difference between our calculated J_{max} in ghost and V_{max} in adipocytes may largely be explained by the temperature effect. Assays also at 5°C, 10°C and 15°C show that the activation energy of k_3^* is 103 ± 4.5 kJ mol^{-1} [8], little different from 125 kJ mol^{-1} of chloride exchange [33]. On this basis, we expect in the ghosts a J_{max} 24-fold higher at 23°C and 135-fold higher at 37°C provided the capacity is temperature independent. Thus it appears that the membrane of the ghost and of the three other cell types are not greatly differently equipped with a transport system. This result is intriguing since the erythrocytes process fatty acids only in acylation-deacylation cycles [34,35]. It brings up the question whether the transport is secondary to another more important transport.

The work of Abumrad et al. [3] shows a dose dependent block of the transport by the anion transport blocker DIDS. This is interesting since 1 g human 'ghosts' (about 10^{10} cells) has about 5–29 nmoles of the anion transporter [26], which almost coincides with the palmitate binding capacity (19 nmoles). However, we are unable to observe any effect of DIDS neither on the efflux of palmitate from the ghosts, nor on the uptake. Without identification of the palmitate binder it can not be excluded that the same transporter is responsible for both the transfer of palmitate and the 10^4-fold greater exchange flux of chloride [17] since the translocation mechanisms of chloride and palmitate must be entirely different. The obvious objection to this speculation is that DIDS blocks both functions in adipocytes. However, this and related problems underscore the need of investigations of the transporters of different cells. They may well be different proteins which have the binding and the translocation of long chain fatty acids in common. A considerable diversity is known for anion- as well as for the glucose-transporter [36].

Acknowledgements

P.J. Bjerrum, J. Funder and J. Brahm, Institute of General Physiology and Biophysics, University of Copenhagen, have introduced us to the ghost technique. M. Crone and J. Salomonsen, Institute of experimental Immunology, University of Copenhagen, have prepared ^{125}I-albumin. E. Sjøntoft, Institute of experimental Surgery, University of Copenhagen, has carried out analyses by the Gauss-Newton least-squares procedure. I. Jørgensen provided skilful technical assistance and K. Olsen has prepared the manuscript. All these contributions are gratefully acknowledged. We particularly wish to thank P.J. Bjerrum and J. Sturis, Physics Laboratory III, The Technical University of Denmark, for many helpful discussions. The work was supported by grant 12-6837, from The Danish Medical Research Council and by a grant from the NOVO-Foundation, Copenhagen, Denmark.

References

1 Bojesen, I.N. and Bojesen, E. (1989) Acta Endocrinol. 120, 459–465.
2 Bito, L.Z. and Baroody, R.A. (1975) Am. J. Physiol. 229, 1580–1584.
3 Abumrad, N.A., Park, J.H. and Park, C.R. (1984) J. Biol. Chem. 259, 8945–8953.
4 Schwieterman, W., Sorrentino, D., Potter, B.J., Rand, J., Kiang, C.-L., Stump, D. and Berk, P.D. (1988) Proc. Natl. Acad. Sci. U.S.A. 85, 359–363.
5 Sorrentino, D., Stump, D., Potter, B.J., Robinson, R.B., White, R., Kiang, C.-L. and Berk, P.D. (1988) J. Clin. Invest. 82, 928–935.
6 Stremmel, W. (1989) Mol. Cell. Biochem. 88, 23–29.
7 Stremmel, W., Strohmeyer, G. and Berk, P.D. (1986) Proc. Natl. Acad. Sci. U.S.A. 83, 3584–3588.
8 Bojesen, I.N. and Bojesen, E. (1990) Mol. Cell. Biochem. 98, 209–215.
9 Bröring, K., Haest, C.W.M. and Deuticke, B. (1989) Biochem. Biophys. Acta 986, 321–331.
10 Chen, R.F. (1967) J. Biol. Chem. 242, 173–181.
11 Markwell, M.A.K. and Fox, C.F. (1978) Biochemistry 17, 4807–4817.
12 Scheider, W. (1979) Proc. Natl. Acad. Sci. U.S.A. 76, 2283–2287.
13 Landaw, E.M. and DiStefano III, J.J. (1984) Am. J. Physiol. 246, R665–R677.
14 Bojesen, E. and Bojesen, I.N. (1986) Scand. J. Clin. Lab. Invest. 46, 1–17.
15 Beck, J.V. and Arnold, K.J. (1977) Parameter Estimation in Engineering and Science, John Wiley and Sons, New York.
16 Schwoch, G. and Passow, H. (1973) Mol. Cell. Biochem. 2, 197–218.
17 Funder, J. and Wieth, J.O. (1976) J. Physiol. 262, 679–698.
18 Van Kampen, E.J. and Zijlstra, W.G. (1961) Clin. Chim. Acta 6, 538–544.
19 Bojesen, I.N. (1985) Prostaglandins 30, 479–489.
20 Bojesen, E. and Bojesen, I.N. (1982) Acta Physiol. Scand. 114, 513–522.

21 Dalmark, M. and Wieth, J.O. (1972) J. Physiol. 224, 583–610.
22 Spector, A.A. (1975) J. Lipid Res. 16, 165–179.
23 Spector, A.A. and Fletcher, J.E. (1978) in Disturbances in Lipid and Lipoprotein Metabolism (Dietschy, J.M., Gotto Jr., A.M. and Ontho, J.A., eds.), pp. 229–249, American Physiology Society, Bethesda, MD, U.S.A.
24 Wilkinson, G.N. (1961) Biochem. J. 80, 324–332.
25 Goodman, D.S. (1958) J. Clin. Invest. 37, 1729–1735.
26 Knauf, P.A. (1979) in Current Topics in Membranes and Transport (Bronner, F. and Kleinzeller, A., eds.), Vol. 12, pp. 250–363, Academic Press, New York.
27 Deuticke, B. (1977) Rev. Physiol. Biochem. Pharmacol. 78, 1–97.
28 Rooney, E.K., East, J.M., Jones, O.T., McWhirter, J., Simmonds, A.C. and Lee, A.G. (1983) Biochim. Biophys. Acta 728, 159–170.
29 Spector, A.A., Ashbrook, J.D., Santos, E.C. and Fletcher, J.E. (1972) J. Lipid Res. 13, 445–451.
30 Svenson, A., Holmer, E. and Anderson, L.O. (1974) Biochim. Biophys. Acta 342, 54–59.
31 Brown, J.R. and Shockley, P. (1982) in Lipid Protein Interactions, Vol. 1 (Jost, P.C. and Griffith, O.H., eds.), pp. 25–68, John Wiley and Sons, New York.
32 Taverna, R.D. and Langdon, R.G. (1973) Biochim. Biophys. Acta 298, 412–421.
33 Brahm, J. (1977) J. Gen. Physiol. 70, 283–306.
34 Mulder, E. and Van Deenen, L.L.M. (1965) Biochim. Biophys. Acta 106, 106–117.
35 Staufenbiel, M. (1987) Mol. Cell. Biol. 7, 2981–2984.
36 Lodish, H.F. (1986) Harvey Lect. 82, 19–46.
37 Stiles, J.W., Francendese, A. and Masoro, E.J. (1975) Am. J. Physiol. 229, 1561–1568.
38 Bengtsson, B.G., Kiessling, K.H., Smith-Kielland, A. and Morland, J. (1981) Eur. J. Biochem. 118, 591–597.
39 Hewett, K., Legato, M.J., Danilo, P. and Robinson, R.B. (1983) Am. J. Physiol. 245, H830–H839.